Proceedings of the ASME 2016 Dynamic Systems and Control Conference
DSCC 2016
October 12-14, 2016, Minneapolis, Minnesota, USA

DSCC2016-9851

A Control Framework for Anthropomorphic Biped Walking Based on Stabilizing Feedforward Trajectories

Siavash Rezazadeh and Robert D. Gregg
Department of Bioengineering, University of Texas at Dallas
Richardson, TX 75080, USA
Email: {siavash.rezazadeh, rgregg}@utdallas.edu

ABSTRACT

Although dynamic walking methods have had notable successes in control of bipedal robots in the recent years, still most of the humanoid robots rely on quasi-static Zero Moment Point controllers. This work is an attempt to design a highly stable controller for dynamic walking of a human-like model which can be used both for control of humanoid robots and prosthetic legs. The method is based on using time-based trajectories that can induce a highly stable limit cycle to the bipedal robot. The time-based nature of the controller motivates its use to entrain a model of an amputee walking, which can potentially lead to a better coordination of the interaction between the prosthesis and the human. The simulations demonstrate the stability of the controller and its robustness against external perturbations.

INTRODUCTION

State-of-the-art control of humanoid robots chiefly relies on methods based on Zero Moment Point (ZMP) [1] which generally result in quasi-static, inefficient, and unnatural walking gaits. Although several successful attempts on the implementation of dynamic locomotion on the bipedal robots have been reported in the past years [2–5], still a fully dynamic and human-like locomotion of an anthropomorphic robot has yet to be achieved. The highly stable, robust, dynamic, efficient, and natural-looking walking achieved with ATRIAS in 3D [5] motivated us to extend the method to a more human-like system. Although ATRIAS was designed to capture the essence of biological walking through dynamics of Spring-Loaded Inverted Pendulum (SLIP) [6], features such as use of large springs, very light legs, and lack of feet and ankle actuation make it different from human/humanoid dynamics in lower layers of the control.

In the present work, we rely on the same control philosophy as introduced in [7], which was based on finding paradigms with strong stabilizing effects at the reduced-order-model level. The strong stabilizing effect of such strategies makes them robust against uncertainties and unmodeled dynamics which are often the main causes of walking failure. The method utilized here is based on time-based feedforward trajectories for knee and ankle which require almost no sensor information and as a result, has minimum sensitivity to noise and faulty feedbacks. Since the stabilization effect of these trajectories requires compliance in the system, they are implemented using human-inspired impedance controllers to provide the required behavior.

The structure of the controller, as well as the fact that it is designed for a human-like model, makes it appropriate for a related application; namely powered prosthetic legs. The proposed methods for the active control of tranfemoral prostheses can generally be divided into impedance control (as in [8]) and virtual constraint control [9]. Both of these methods rely on the reactive response (kinematically or kinetically) of the prosthetic leg to the amputee's motion. Inspired by the time-based foundation of the controller and the fact that entrainment is a widely present phenomenon in biological systems, in the latter part of this work, we investigate the possibility of using the proposed controller for the prosthetic leg for entraining purposes. This can potentially lead to a coordinated cooperation of the healthy and prosthetic legs to achieve a stable walking gait.

The paper is organized as follows. First, a dynamic model of the bipedal system reasonably close to that of the humans is presented and its Lagrangian dynamics are formulated. Next, the controller for the biped model is constructed and presented. Having the controlled dynamics of the robotic biped, its

performance in conditions such as high initial condition errors as well as external perturbations is simulated and investigated. As an alternative application of the controller, in the next section, we investigate the case that the legs have different controllers and the ability of the prosthesis to entrain the human motion. Finally, in the Conclusion section, we discuss about the lessons taken from this study and provide suggestions for future works.

DYNAMIC MODEL

Figure 1 depicts a schematic of the model considered for dynamic formulation and simulation. The model has been chosen to be able to model a reasonably close approximation of the dynamics of a human's or a humanoid robot's walking in the sagittal plane. The lengths and masses used are according to the average fractions of the body height and total body mass as in pp. 60, 63, and 64 of [10]. The upper body (torso, arms, head) are modelled as a single rigid body. There are a total of six actuators (three per leg) which are modeled as electric motors (with inertia and damping) in series with a transmission with a constant gear ratio, driving the leg joints (hip, knee, and ankle).

Taking $q = [x, y, \theta_h^R, \theta_k^R, \theta_a^R, \theta_h^L, \theta_k^L, \theta_a^L, \theta_b]^T$, where x and y are the horizontal and vertical coordinates of the hip joint with respect to the world, and superscripts R and L represent the right and the left leg, respectively, the free floating Lagrangian dynamics of the system can be written as:

$$D(q)\ddot{q} + C(q,\dot{q})\dot{q} + G(q) = A^T u + J^T F \qquad (1)$$

where $u \in \mathbb{R}^6$ is the control input vector (motor torques), F contains the Ground Reaction Forces (GRF), and $A_{6\times9}$ and J are appropriate Jacobian matrices.

In order to obtain the GRF, commonly the foot touchdown is assumed to be an inelastic impact process [7,11]. However, as shown in [12,13], in some situations the conditions for inelastic impact cannot be satisfied and the leg will inevitably slip along the surface. Therefore, in the present work, we adopt the method presented in [14] (Eq. (35)), which suggests a nonlinear compliant contact model for the interaction of the feet with the surface. This also has the advantage of eliminating the necessity for multiple phases (heel-contact, flat-foot, toe-contact, swing; see for example [15]) which makes the simulation faster and simpler. Note that in our model, the feet are considered as two-point-contact elements (heel and toe), each point having horizontal and vertical forces, which makes F a vector in $\mathbb{R}^8$, and correspondingly, J an 8×9 matrix.

CONTROL DESIGN

The controller proposed in [5] was based on using an oscillator in series with a compliant element (spring-damper) as depicted in Figure 2. As shown in [5], selecting x_m as an appropriate feedforward periodic (time-based) function will lead to globally stable oscillations of the spring-mass system. This is a powerful paradigm, for several reasons, including: 1) there is no need for feedback, and as a result, the system is not sensitive to measurement errors; 2) global stability is highly beneficial for a dynamic phenomenon such as walking in which starting from a wide range of initial conditions should be possible; and 3) in the case of robots with series elastic actuation (such as ATRIAS), controlling x_m is equivalent to position control of the motors, which can be achieved utilizing simple (yet robust) controllers such as Proportional-Derivative (PD) control.

The ability of this reduced-order-model-based control paradigm for control of a full-order robot has been shown in [5]. This fact motivates us to pursue the extension of it to more complicated cases such as the system shown in Figure 1. In general, the anthropomorphic model of Figure 1 has five main differences from a robot specifically designed to match the spring-mass model such as ATRIAS [16]; namely: 1) flat feet instead of point feet; 2) ankle actuation; 3) lack of compliant element; 4) legs with non-negligible masses; and 5) taller torso. Among these differences, numbers 4 and 5 (the leg mass and torso center of mass position) are essentially handled through robustness of the control algorithm and tuning. The other differences are addressed in the controller design as it is discussed in what follows.

Feedforward Time-Based Scheme

For the reduced-order model of Figure 2, the only time-based variable is the input in leg length direction (x_m), which essentially balances the energy lost through damping to achieve a stable set of oscillatory motions. Taking the period for one stride as $2T$ (to imply a symmetric gait with T for each step), it is equivalent to: $x_m(t) = x_m(t + 2T)$.

For the full-order model (Figure 1), similar to [5] the desired knee trajectory for one leg can be taken as:

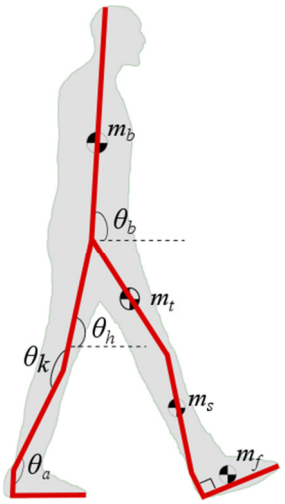

Figure 1. The model used for the formulation of walking dynamics

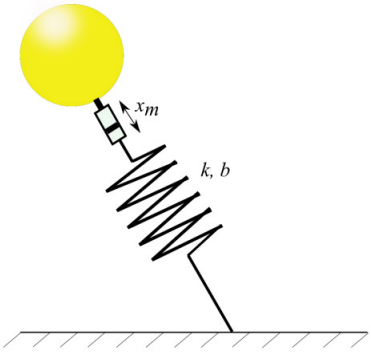

Figure 2. Actuated spring-mass model with damping

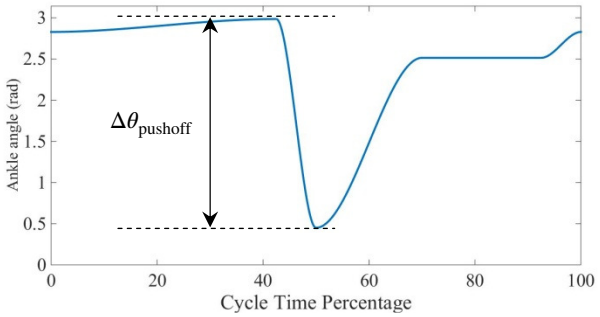

Figure 3. Desired reference trajectory for ankle angle during one cycle where roughly the first half corresponds to stance phase and the second half to swing phase.

$$\theta_{k,d} = \begin{cases} \theta_{k,0} - \theta_{ret}\sin\left(\frac{\pi}{T}t\right), & \sin\left(\frac{\pi}{T}t\right) > 0 \\ \theta_{k,0}, & \sin\left(\frac{\pi}{T}t\right) \le 0 \end{cases} \quad (2)$$

where $\theta_{k,0}$ is a constant representing the reference knee angle, and θ_{ret} is the maximum retraction angle in swing phase. In equation (2), the leg retraction and protraction phases are of the same duration ($T/2$). However, in practice the sinusoidal trajectory can be replaced by any other smooth trajectory for reasons such as faster retraction and smoother protraction.

Similar to the knee trajectory, the ankle trajectory is designed to facilitate both natural walking and stabilization. The two important factors required to be considered for the ankle trajectory are ankle push-off at the end of the stance, and dorsiflexion at the beginning of swing phase to accommodate the desired foot clearance.

Figure 3 shows an example of such reference trajectory for ankle angle which will be used in this work. It essentially consists of four different sections whose start and end point are connected using cubic splines. The sudden fall in the middle part of the trajectory corresponds to push-off at the end of the stance phase. Before that and throughout stance, the reference trajectory is almost constant (there is a small shift according to what observed in human walking as reported in [17]), which means that the ankle essentially behaves as a spring, slightly resisting the motion and through that storing energy to be released in push-off. During swing phase and after the initial dorsiflexion, the ankle angle remains constant until right before the end of the cycle, when it increases slightly further to prepare for touchdown and the next stance phase.

Note that most of the considerations in designing this trajectory are purely geometrical and do not affect the stability of the system. Since the change in dynamics parameters of the system (masses, frictions, etc.) will have very minor effects on the geometrical constraints, the suggested trajectory remains chiefly unchanged in the case of such changes. The main factor impacting the dynamic stability is the magnitude of the push-off, which is a determining factor for regulating the energy of the gait. As such, the change of the reference ankle angle in push-off is proposed to be a function of the desired walking speed (Figure 3):

$$\Delta\theta_{\text{pushoff}} = c_1 + c_2 v_d \quad (3)$$

Knee/Ankle Actuation: Impedance Control

The stable oscillations of the model of Figure 2 are achieved through the interaction of the feedforward input with a compliant element. For a rigid robot (or prosthetic leg) this compliance has to be simulated through impedance control [18]. When joint-level torque control is possible, it can be utilized for elimination of motor dynamic effects (inertia, etc.) and replication of the desired behavior of a spring-damper system. However, in the present research we consider the stricter condition in which the joint-level control is not available. In this case, the motor dynamics are present and become part of the dynamics of the system (so long as the actuator has some backdriveability and allows motion induced from the joint side). In this case, the motor torque (control input), u_m, can be obtained from the following general form:

$$u_m = c(t, v_d)\left[k_1(\theta_d - \theta) + k_2\left(\dot{\theta}_d - \dot{\theta}\right)\right] \quad (4)$$

which is essentially a PD controller with variable gains which depend on time (t) and the desired walking speed (v_d). Note that the reference trajectories, θ_d, are the ones discussed in the previous subsection (e.g. equation (2)).

For a model with feet and ankle actuation (Figure 1) the leg length actuation is divided between knee and ankle joints. In humans, the GRF in the first half of stance is mainly produced by the knee, whereas in the second half the ankle is the major source of the force (cf. joint torque diagrams in [10]). Accordingly, the knee gains are decreased during stance while the ankle gains are increased.

Hip Actuation: Foot Placement and Torso Pitch Control

Hip actuators serve for two different purposes during stance and swing. During stance they work to counteract the

knee and ankle actuation to maintain the torso close to upright, while during swing, it controls the placement of the foot to provide the right initial condition for the next stance phase.

In the design of the hip control for these two purposes we follow the analysis by Qiao and Jindrich [19] wherein using experimental data they showed that Raibert's controllers for torso pitch control and foot placement [20] have good correlations with experimental data of human walking.

The Raibert control for regulating torso pitch is essentially a PD controller:

$$u_h = k_P\left(\frac{\pi}{2} - \theta_b\right) - k_D\dot{\theta}_b \tag{5}$$

where u_h is the hip torque and k_P and k_D are positive constants.

In swing phase, Raibert suggests to use foot placement to regulate the walking speed [20]:

$$x = a_1 v + a_2(v - v_d) \tag{6}$$

where x is distance between the foot and the center of mass, and a_1 and a_2 are positive gains.

Note that for control of ATRIAS, for both torso control and foot placement, more sophisticated controllers were designed [5]. In particular, foot placement algorithm was based on a discrete PID control of the walking speed and torso control was performed using feedback linearization. These algorithms can certainly be applied in our framework, as well. However, in the present work, with an eye on application in control of prosthetic legs, we try to find the simplest control for the hip actuation (which in the case of prosthetic legs is controlled by the amputee), in order to achieve a fundamentally similar behavior to human controls (although they may quantitatively differ). The study of other types of hip joint control is left to future works.

WALKING SIMULATION

Using the controller presented and discussed in the previous section, the dynamic response of the system of Figure 1 is simulated in MATLAB® for a subject with height and weight of 1.80 m and 80 kg, respectively. Body segment heights and weights and the locations for CoM's are calculated according to approximations provided in [10]. All motors are considered to be of the same type with inertia of $1\mathrm{e}-4\ \mathrm{kg\cdot m^2}$ and damping coefficient of $1\mathrm{e}-5\ \mathrm{N\cdot s/m}$ (typical values). The gear ratios are assumed to be 100. The period of oscillations for the feedforward terms is $2T = 1$ s.

In order to demonstrate the stability of the proposed controller, the mechanism is released from the heels being 10 cm above the ground. It is expected to balance itself after contact with the ground, start walking, and converge to a stable limit cycle. The desired walking speed is 1 m/s. Figure 4 depicts the hip velocity throughout this simulation. As can be seen from the figure, after being released at the start of the simulation, the system takes a few steps backward until it gains enough energy to move forward and then converges to a limit cycle with a walking speed reasonably close to the desired speed (1 m/s). Figure 5 depicts the phase portrait for the vertical motion of the hip and Figure 6 shows the stick diagram for one cycle of the legs (two steps of walking).

To investigate the stability of the walking controller against external disturbances, a horizontal force pulse of 200 N for the duration of 1 s is applied to the biped system at the hip. As can be observed in Figure 7, the force changes the velocity to -1.4 m/s (negative sign for backward motion), but the system is able to recover from this disturbance and return to its stable walking within a few steps.

ENTRAINMENT AND APPLICATION IN THE CONTROL OF ACTIVE PROSTHETIC LEGS

As mentioned before, control of powered prosthetic legs for transfemoral amputees relies either on simulating the compliance of the human joint through impedance control [8], or following the kinematic trajectories of the joints using virtual constraints [9,21]. Both these methods assume the dynamics of the prosthesis and its interaction with the human body is the same as a human leg. However, in general, this is not true, and it can be one of the main reasons that, for example, the tuned impedance parameters of the controller presented in [8] are significantly different from those of the humans. Theoretically, the only way for the prosthesis to induce the same walking as a healthy leg is to control the socket interaction forces to match those of the healthy leg. Due to major difficulties accompanied with this, we propose another approach to the problem, namely entrainment.

Entrainment, the synchronization of two (or more) frequencies due to a weak interaction, has been observed in various biological phenomena. Taga proposed a control paradigm for walking based on the entrainment of neural oscillators (famously known as Central Pattern Generation - CPG) [22], which has been the basis of numerous works on locomotion control ever since [23]. Although the role of CPG in human walking remains a point of contention [24], Ahn and Hogan showed that the frequency of walking in healthy subjects adapts itself to rhythmic pulses from an external actuator on the ankle [25]. The small basin of entrainment observed in their experiments can be attributed to characteristics of a stable nonlinear oscillator underlying human walking. Motivated by this result, in what follows, we study the possibility of using entrainment for inducing a stable set of oscillations in the human+prosthesis system (rather than trying to imitate the original oscillator).

In order to investigate the feasibility of the controller presented in the previous section for prosthetic legs, we assume two different control paradigms for healthy and amputated legs. For the healthy leg, we rely on the work by Villarreal et al. wherein through statistical analysis of perturbed human walking data, it is shown that the best correlation between nominal and perturbed trajectories are given when the gait is parameterized using hip phase angle [26]. The controller designed based on this new parameterization has resulted in robust walking with a powered prosthetic leg [21]. Inspired by this finding, we re-parameterize the controls for the knee and

the ankle of one of the legs to replace time with the hip phase angle. From [26], the normalized hip phase angle for a specific limit cycle can be computed from:

$$\phi = \frac{\arctan2\left[\frac{-\left|\max(\theta_{h,v}) - \min(\theta_{h,v})\right|}{\left|\max(\dot{\theta}_{h,v}) - \min(\dot{\theta}_{h,v})\right|}\dot{\theta}_{h,v}, \theta_{h,v}\right]}{2\pi} \quad (7)$$

which gives a value in the [0,1] interval. $\theta_{h,v} = \frac{\pi}{2} - \theta_h$ is the thigh angle with respect to the vertical direction. Note that in the original knee and ankle controller, the parameterizing variable, t_i, can be obtained from:

$$t_i = t \bmod 2T \quad (8)$$

Then, performing the replacement:

$$t_i \longrightarrow 2T \cdot \phi \quad (9)$$

will be equivalent to the re-parameterization of the controller in terms of hip phase angle.

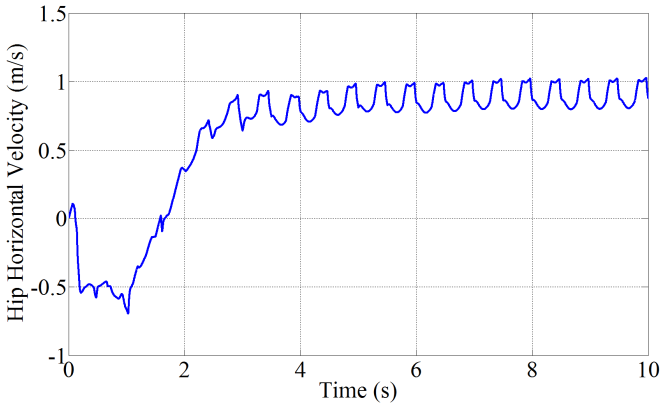

Figure 4. The horizontal velocity of the hip for the system released from 10 cm above the ground converges to a limit cycle with the desired velocity (1 m/s).

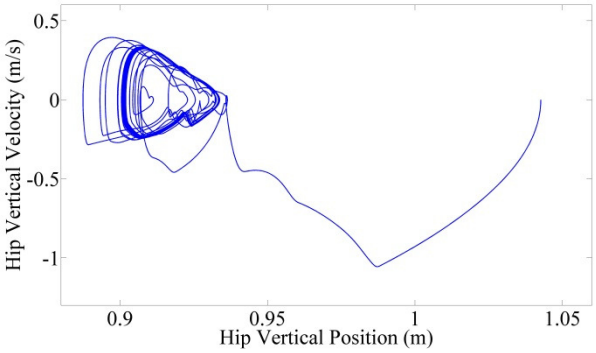

Figure 5. Phase portrait for the hip's vertical motion during the walking simulation. The trajectory converges to a stable limit cycle after a few oscillations.

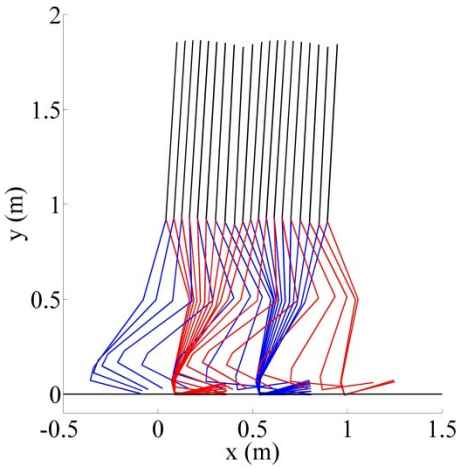

Figure 6. Stick diagram of one cycle (stride) of the legs (1 second).

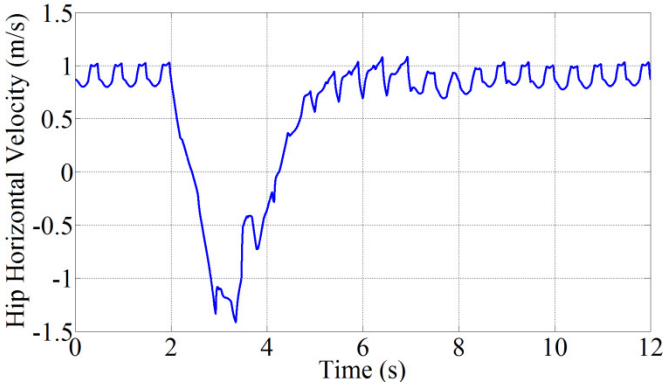

Figure 7. The response to a perturbation force of 200 N for 1 s (starting at $t = 2$ s). After some transients, the system is able to go back to its stable limit cycle.

Using this change of parameterization, we simulated the system to start from a point on the limit cycle found previously, and observed the change in the resulted trajectories. First, the simulation is done with $2T = 1$ s for the prosthetic leg (as in the previous section) and then with $2T = 1.02$ s to study the entrainment. As can be seen in Figure 8, in both cases the difference between the frequency of the dynamic response of the system and the feedforward frequency of the prosthetic leg (the entraining signal) converges to zero. This is equivalent to synchronization of the two legs. Note that, as it is depicted in Figure 9, the system no longer converges to a symmetric (period-1) limit cycle. This is expected, as the controllers for the two legs are different. But as mentioned before, it is interesting that regardless of this asymmetry, the periods for the two legs converge to equal values. Indeed, this effect can be minimized using parameter tuning.

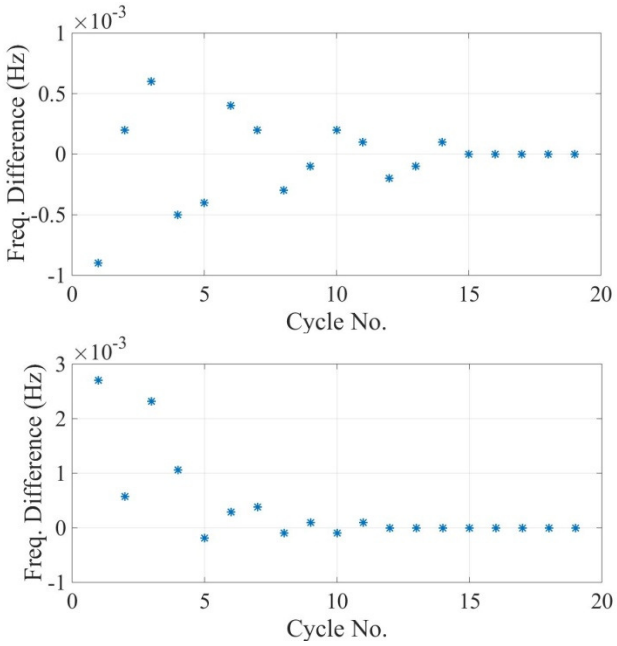

Figure 8. Entrainment of one leg based on time-based control of the other leg. **Top:** $2T = 1$ s. **Bottom:** $2T = 1.02$ s. In both cases the frequency of entrained leg eventually converges to that of the controlled leg.

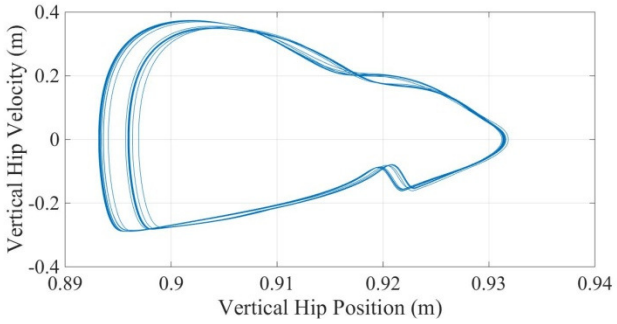

Figure 9. The system converges to a period-2 limit cycle with entrainment.

CONCLUSION

A method for control of humanoid robots and tranfemoral prostheses based on designing feedforward time-based trajectories for the knee and the ankle. Previously, the stabilizing effects of these trajectories in interaction with compliant elements had been demonstrated in [5]. We extended the method to a human-like model with no compliant components. It was shown that these trajectories together with impedance control of the actuators (to simulate compliance) even in the absence of joint torque feedback can result in highly stable walking. Compared to classic control methods of humanoids such as ZMP, the proposed approach results in faster, more natural-looking, more dynamic (and as a result, more efficient) bipedal walking.

This potentially can open new doors to better understanding of human walking and the highly stable and efficient characteristics that it exhibits. In particular, instead of methods relying heavily on detailed models which (unlike humans) makes them vulnerable to uncertainties and disturbances, we propose to use strong stabilizing paradigms that can preserve their effects in the face of uncertainties and unmodeled dynamics by simple tunings.

Inspired by these facts and as another application, we investigated the control of powered prostheses for tranfemoral amputees using the proposed controller. Considering the human walking as a nonlinear oscillator, we showed that the controller is able to entrain the amputee model to a new stable set of oscillations. As an attempt to achieve a coordinated stable interaction between the prosthesis and the amputee, we believe this approach can result in an improved quality of walking, compared to the current methods which are based on reactive response and imitation of normal walking.

In the next stages of this research, we intend to test the method by performing experiments on a humanoid robot as well as a prosthetic leg to verify its stability and the ability of entrainment (for the latter case). Specifically for prosthesis control, it is necessary to consider issues such as changing the settings of the induced oscillations based on feedback from the subject's hip angle/velocity (for example when the subject is standing the prosthesis should not be oscillating). Furthermore, the controller can be extended and tested for other maneuvers such as faster speeds, running, and walking up and down stairs. This can lead to a better understanding of the method as well as its relation with the mechanisms humans use for locomotion.

ACKNOWLEDGMENTS

The authors would like to thank Dr. Kaveh Akbari Hamed from the San Diego State University for his kind help and valuable consultation.

This work was also supported by the Eunice Kennedy Shriver National Institute of Child Health & Human Development of the National Institutes of Health under Award Number DP2HD080349. The content is solely the responsibility of the authors and does not necessarily represent the official views of the NIH. Robert D. Gregg, IV, Ph.D., holds a Career Award at the Scientific Interface from the Burroughs Wellcome Fund.

REFERENCES

[1] Vukobratovic, M., and Juricic, D., 1969, "Contribution to the Synthesis of Biped Gait," IEEE Trans. Biomed. Eng., **BME-16**(1), pp. 1–6.

[2] Bhounsule, P. A., Cortell, J., Grewal, A., Hendriksen, B., Karssen, J. G. D., Paul, C., and Ruina, A., 2014, "Low-bandwidth reflex-based control for lower power walking: 65 km on a single battery charge," Int. J. Rob. Res., **33**(10), pp. 1305–1321.

[3] Sreenath, K., Park, H.-W., Poulakakis, I., and Grizzle, J. W., 2010, "A Compliant Hybrid Zero Dynamics

Controller for Stable, Efficient and Fast Bipedal Walking on MABEL," Int. J. Rob. Res., **30**(9), pp. 1170–1193.

[4] Sreenath, K., Park, H.-W., Poulakakis, I., and Grizzle, J., 2013, "Embedding active force control within the compliant hybrid zero dynamics to achieve stable, fast running on MABEL," Int. J. Rob. Res., **32**(3), pp. 324–345.

[5] Rezazadeh, S., Hubicki, C. M., Jones, M., Peekema, A., Van Why, J., Abate, A., and Hurst, J., 2015, "Spring-mass Walking with ATRIAS in 3D: Robust Gait Control Spanning Zero to 4.3 KPH on a Heavily Underactuated Bipedal Robot," Proceedings of the ASME 2015 Dynamic Systems and Control Conference ASME/DSCC 2015, ASME, p. V001T04A003.

[6] Blickhan, R., 1989, "The spring-mass model for running and hopping," J. Biomech., **22**(11-12), pp. 1217–1227.

[7] Rezazadeh, S., and Hurst, J. W., 2015, "Toward step-by-step synthesis of stable gaits for underactuated compliant legged robots," Proceedings - IEEE International Conference on Robotics and Automation, IEEE, Seattle, USA, pp. 4532–4538.

[8] Sup, F., Bohara, A., and Goldfarb, M., 2008, "Design and Control of a Powered Transfemoral Prosthesis.," Int. J. Rob. Res., **27**(2), pp. 263–273.

[9] Gregg, R. D., Lenzi, T., Hargrove, L. J., and Sensinger, J. W., 2014, "Virtual constraint control of a powered prosthetic leg: From simulation to experiments with transfemoral amputees," IEEE Trans. Robot., **30**(6), pp. 1455–1471.

[10] Winter, D. A., 2005, Biomechanics and Motor Control of Human Movement, John Wiley & Sons.

[11] Grizzle, J. W., Abba, G., and Plestan, F., 2001, "Asymptotically stable walking for biped robots: analysis via systems with impulse effects," IEEE Trans. Automat. Contr., **46**(1), pp. 51–64.

[12] Keller, J. B., 1986, "Impact With Friction," J. Appl. Mech., **53**(1), pp. 1–4.

[13] Hurmuzlu, Y., and Marghitu, D. B., 1994, "Rigid Body Collisions of Planar Kinematic Chains With Multiple Contact Points," Int. J. Rob. Res., **13**(1), pp. 82–92.

[14] Plestan, F., Grizzle, J. W., Westervelt, E. R., and Abba, G., 2003, "Stable walking of a 7-dof biped robot," IEEE Trans. Robot. Autom., **19**(4), pp. 653–668.

[15] Lv, G., and Gregg, R. D., 2015, "Orthotic Body-Weight Support Through Underactuated Potential Energy Shaping with Contact Constraints," Proc. IEEE Conf. Decis. Control / IEEE Control Syst. Soc. IEEE Conf. Decis. Control, (Cdc), pp. 1483–1490.

[16] Grimes, J. A., and Hurst, J., 2012, "The Design of ATRIAS 1.0 a Unique Monopod, Hopping Robot," International Conference on Climbing and Walking Robots (CLAWAR), Baltimore, USA, pp. 548–554.

[17] Shamaei, K., Cenciarini, M., and Dollar, A. M., 2011, "On the mechanics of the ankle in the stance phase of the gait," Proceedings of the Annual International Conference of the IEEE Engineering in Medicine and Biology Society, EMBS, IEEE, pp. 8135–8140.

[18] Hogan, N., 1985, "Impedance Control: An Approach to Manipulation: Part I—Theory," J. Dyn. Syst. Meas. Control, **107**(1), p. 1.

[19] Qiao, M., and Jindrich, D. L., 2012, "Task-Level Strategies for Human Sagittal-Plane Running Maneuvers Are Consistent with Robotic Control Policies," PLoS One, **7**(12).

[20] Raibert, M. H., 1986, Legged robots that balance, Massachusetts Institute of Technology.

[21] Quintero, D., Villarreal, D. J., and Gregg, R. D., 2016, "Preliminary Experiments with a Unified Controller for a Powered Knee-Ankle Prosthetic Leg Across Walking Speeds," IEEE Int. Conf. on Intelligent Robots and Systems.

[22] Taga, G., Yamaguchi, Y., and Shimizu, H., 1991, "Self-organized control of bipedal locomotion by neural oscillators in unpredictable environment," Biol. Cybern., **65**(3), pp. 147–159.

[23] Ijspeert, A. J., 2008, "Central pattern generators for locomotion control in animals and robots: a review.," Neural Netw., **21**(4), pp. 642–53.

[24] Ahn, J., and Hogan, N., 2012, "A Simple State-Determined Model Reproduces Entrainment and Phase-Locking of Human Walking," PLoS One, **7**(11), p. e47963.

[25] Ahn, J., and Hogan, N., 2012, "Walking Is Not Like Reaching: Evidence from Periodic Mechanical Perturbations," PLoS One, **7**(3), p. e31767.

[26] Villarreal, D. J., Poonawala, H. A., and Gregg, R. D., 2016, "A Robust Parameterization of Human Gait Patterns Across Phase-Shifting Perturbations," IEEE Trans. Neural Syst. Rehabil. Eng.